

On the investigation of separation between reflection and backscattering components by plane wave imaging for estimation of surface roughness

表面粗さの評価のための平面波イメージングによる反射・散乱成分の分離に関する研究

Kazuhiro Tochigi^{1‡}, Ryo Nagaoka¹, Jens E. Wilhjelm², Hideyuki Hasegawa¹
(¹Univ. Toyama; ²Technical Univ. Denmark)

栃木一宏^{1‡}, 長岡 亮¹, ウィルヘルム イェンス エリック², 長谷川英之¹
(¹富山大学; ²デンマーク工科大学)

1. Introduction

When the endothelial cells on the arterial wall are damaged and detached in the early stage of atherosclerosis, the luminal surface of the blood vessel roughens [1]. When ultrasonic waves are obliquely incident on such a rough surface, the backscattered component becomes stronger compared to when the surface is smooth. Therefore, separation of the reflection component from the backscattering component in the signal from the transducer could be useful for diagnosing early stage atherosclerosis. Previously, we investigated the separation of reflected and backscattered components in echo signals using synthetic aperture methods with spherically diverging waves [2]. In this study, we aimed to separate the reflection and backscattering components by plane wave transmission and to compare the separated signals representing these two components.

2. Principle

2.1. Plane wave imaging

In plane wave imaging, the transmission propagation distance r_t from the center of the transmit aperture to a target point (x_t, z_t) is obtained by

$$r_t = x_t \sin \theta + z_t \cos \theta. \quad (1)$$

Similarly, the receiving propagation distance r_i from the target point to the i -th element in the receiving aperture at $(x_i, 0)$ is obtained by

$$r_i = \sqrt{(x_i - x_t)^2 + z_t^2}. \quad (2)$$

2.2. Method for separation of reflection and scattering components

In this study, an ultrasonic wave is transmitted to the point of interest (x_t, z_t) as illustrated in **Fig. 1** from the $-\theta$ direction. Since the reflection occurs in the θ direction, the center of arrival for the reflected

component is $(x_r, 0)$. The arrival point of the (180°) backscattered component is $(x_b, 0)$ as illustrated in **Fig. 1**. In addition, the 0° component is not compounded by any method other than the conventional method.

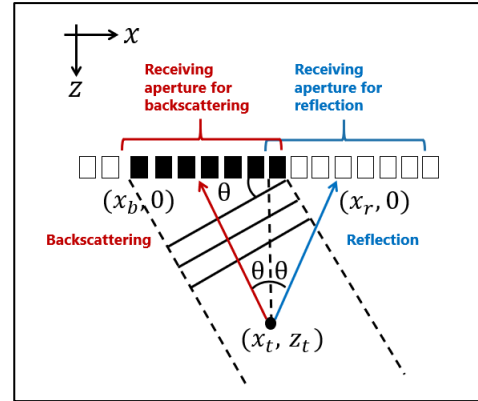


Fig. 1 Schematic of separation of reflection and backscattering components.

2.3. Receive propagation distance for plane sound source

The reflected and backscattered components were attempted separated in the echo signals. Therefore, it is necessary to assume not only a spherical wave but also a plane wave as the returning wave from a target (plane interface) in the receive beamforming. Hence, we also calculate the receive propagation distance when plane waves are returned from a target. As illustrated in **Fig. 2**, when a plane wave just arrives at the element position $(x_e, 0)$, the distance r_i from the position (x_t, z_t) on the surface to $(x_e, 0)$ is obtained by

$$r_i = \sqrt{(x_e - x_t)^2 + z_t^2} \cos(\varphi - \theta). \quad (3)$$

The propagation paths described in Sections 2.1-2.3 were used to perform delay-and-sum beamforming to form a conventional plane wave image, a reflection enhanced image (point and plane sources), and a backscattering enhanced image.

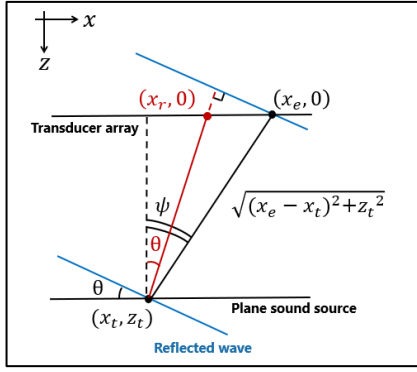


Fig. 2 Schematic of calculation of the receiving propagation distance when assuming a plane sound source.

2.4. Experimental setup

In the experiments, a 192-element linear array transducer with an element pitch of 0.1 mm was used. The center frequency of the transducers was 7 MHz. Ultrasonic echoes received by individual transducer elements were acquired at a sampling frequency of 31.25 MHz. The sound velocity was presumed to be 1482 m/s in the receive beamforming. Three rough and one smooth reflector phantoms with sizes of 10×10 cm were used. These were made of a liquid urethane casting elastomer casted on three grades of sandpaper with decreasing roughness as well as a glass plate [3]. They were denoted P40, P60, P100, and Smooth. The distance from the transducer to each phantom was 10 mm.

3. Results and Discussion

Figs. 3(a)-(d) show for 73 scan lines the maximum amplitude of the echo signal, obtained by conventional plane wave imaging, reflection component, backscatter component, and reflection component by assuming a plane sound source, respectively. Plane waves were transmitted at 5-degree intervals in the range of -20 to 20 degrees. Although 193 scan lines were recorded, only the beams located near the center of the probe were selected to eliminate edge effects. The red lines in Fig. 3 show the averages of the maximum amplitude values for the 73 scan lines. Each plot is normalized individually.

Fig. 4 shows the coefficients of variation (CV) calculated from the means and standard deviations of the maximum amplitude values of the phantoms shown in Fig. 3. In some cases, the values were not continuously increasing with the degree of roughness. In the case of the conventional and the backscattering enhanced images, the drop in the CV

of the P40 phantom is presumably due to the low directivity of the backscattering component. On the other hand, when the reflection component was used to calculate the CV, there was a continuously increase between the surface roughness of the phantom and the CV.

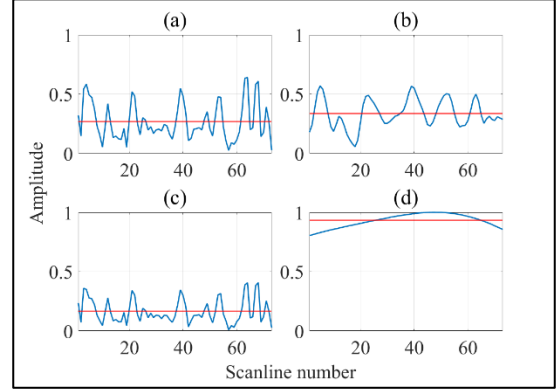


Fig. 3 Amplitude profiles obtained using P100 phantom with (a) conventional plane wave imaging, (b) reflected component, (c) backscattered component, and (d) reflection component assuming a plane reflected wave.

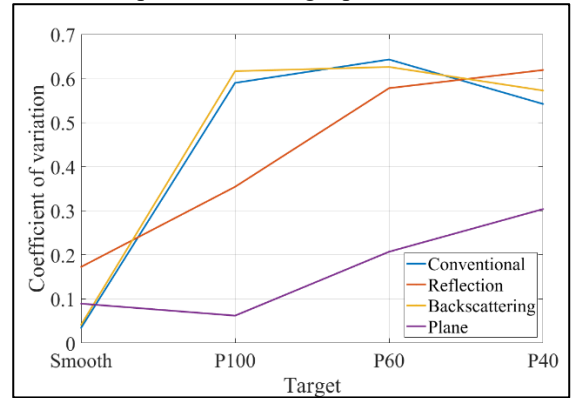


Fig. 4 Coefficients of variation of echo amplitudes acquired in individual scan lines.

4. Conclusions

In this study, the reflection and scattering components were attempted separated in phantom experiments using plane wave imaging and the echo signals for each component were compared. For the reflection component, the CV was continuously increasing with degree of roughness

References

1. E. Sho, M. Sho, T. M. Singh, H. Nanjo, M. Komatsu, C. Xu, H. Masuda, and C. K. Zarins: *Exp. Mol. Pathol.*, **73** (2002) 142.
2. K. Nagata, R. Nagaoka, J. E. Wilhjelm, and H. Hasegawa: *Jpn. J. Appl. Phys.* **60** (2021) SDDE09.
3. J. E. Wilhjelm, P. C. Pedersen, and S. M. Jacobsen: *IEEE Trans. UFFC* **48** (2001) 511.